INTL JOURNAL OF ELECTRONICS AND TELECOMMUNICATIONS, 2019, VOL. 65, NO. 2, PP. 181–187
Manuscript received September 26, 2018; revised April, 2019. DOI: 10.24425/ijet.2019.126299

A New Frequency Reconfigurable Antenna Using Proximity Fed Technique for Wireless Applications

Aziz El Fatimi, Seddik Bri, and Adil Saadi

***Abstract*—This electronic paper presents an innovative technology for efficient use of the radio spectrum. This new frequency reconfigurable rotatable antenna is intended for wireless applications such as WLAN, WiMAX and Bluetooth mobile applications. The working principle of this proposed work is to print square patches mounted on the same circular dielectric substrate feed by a proximity coupling to eliminate the noise signal transmission and problems related to interference. The three positions correspond to an operating frequency controlled by a bipolar step-by-step engine. An optimization of the structure using the FEM finite element method as well as a comparison with other structures recently realized are detailed in this paper. The final numerical simulation results are: WLAN 4.95-5.53 GHz (BW = 11%) Gain = 6.06 dBi, WiMAX 3.35-3.75 GHz (BW = 11.2%) Gain = 7.48 dBi and Bluetooth 2.3-2.51 GHz (BW = 8.7%) Gain = 17.78 dBi.**

***Keywords*—Frequency reconfigurable antenna, patch antenna, proximity coupled antenna, rotatable antenna**

I. Introduction

THE new global environment has shown a great importance in frequency-configurable mobile communications systems due to the advantages offered by this technology such as low cost, simplicity and reduces interference from adjacent unused bands [1]–[5].

According to the literature, for creating multiple frequency bands is based on the insertion of slots on the metal parts of the antenna or the employment of several radiating layers [6], [7]. However, these techniques generally engender a mismatch of input impedance especially with the insertion of asymmetric slots [8].

To deal with this problem, other techniques are used to design parametric antennas by changing frequency using external elements (typically a DC voltage or current) switchable in the antenna structure, like the PIN diodes [3], [4], the varactor diodes [8], the FET switches [9] or the RF-MEMS [10], [11]. RF-MEMS has a low loss though but its integration is very expensive [12].

Many configurations are used to power micro-strip patch antennas. The popular feeding techniques of antennas are the feed line, the coaxial probe, the opening coupling and the proximity coupling. Each type is used according to the operating environment [13]–[19].

For all patch antenna designs, the conductive feed line is used as a conductive strip. In most cases, the length and the width of the conductive strip are very low compared to the length and the width of the radiating patch. The advantage of this micro-strip line feeding technique is the ease of implementation, easy to adapt by controlling the insertion position and also simple to model. But when the thickness of the dielectric substrate is large, parasitic radiation and surface waves causes a limitation of the width of the bandwidth often between 2 to 5%.

Other types of micro-strip line feeds, there are coaxial feeds that are also widely used. The coaxial probe feed is also simple to manufacture and adapt and has low parasitic radiation. But for thick substrates (h$>0.02\lambda_0$), it also has a small bandwidth and is harder to model.

In this article, a new rotatable antenna fed by electromagnetic proximity coupling is presented, studied, analysed and optimized by a numerical simulation. The designed antenna uses three radiating rectangular patches manipulated by a bipolar step-by-step engine. The following sections study the geometry of the antenna, the parametric analysis of the design and the final results obtained.

II. Ordinary Design of the Proximity-Coupled Structure

To overcome the problems related to narrow bandwidth and parasitic radiation, no contacting feed called proximity coupling feeding has been introduced, as figured in Fig. 1. In the general case, the proximity coupling offers a largest bandwidth with a low parasitic radiation often greater than 13% and it relatively simple to schematize and model. Yet, its realization is very difficult. To control the input characteristic impedance, the stub (feed line inset) length and the ratio between the length and width of the patch can be used to match the impedance to 50 Ω [20].

This technique feeding is also called proximity electromagnetic coupling scheme. The micro-strip line is printed between two dielectric substrates and that the radiating patch is above the upper substrate, as figured in Fig. 1.

The strong advantage of this power method is that it reduce parasitic radiation and provides a large wide bandwidth due to the thickness value of the micro-strip patch antenna substrate. This scheme gives the possibilities to choose between two different dielectric substrates, the first to print the patch and the second to print the power line for easily optimize the performance [21], [22].

Its equivalent circuit for input impedance is shown in Fig. 2.

A. El Fatimi and A. Saadi are with Modeling, Information Processing and Control Systems (MIPCS), National Graduate School of Arts and Crafts, Moulay Ismail University, Meknes, Morocco (e-mails: aziz.elfatimi@edu.umi.ac.ma, rayhan_achraf@yahoo.fr).

S. Bri is with Materials and Instrumentation (MIM), High School of Technology, Moulay Ismail University, Meknes, Morocco (e-mail: brised-dik@gmail.com).).

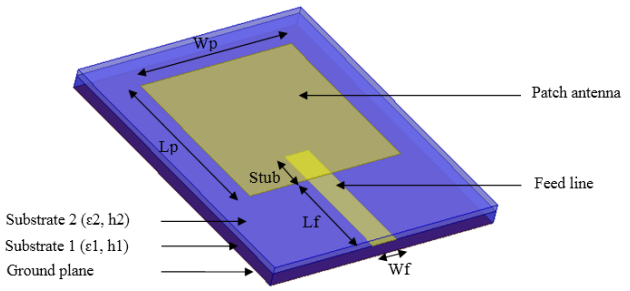

Fig. 1. Typical proximity coupled antenna.

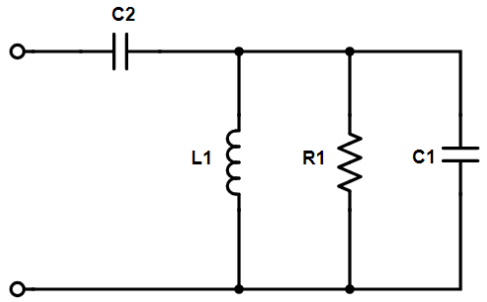

Fig. 2. Equivalent circuit for typical proximity feed.

The C_2 capacitance is called the electromagnetic coupling capacitance between the feed line and the patch antenna [23].

$$C_2 = \frac{W_f.Stub.\epsilon_0.\epsilon_{r2}}{h_2} \tag{1}$$

The feed line between the two dielectric substrates will have fringing fields, which will cause a slight increase in the feed line length. This will create an extra capacity.

Indeed, the stub length of the coupling line affects the signal level coupled to the radiating element. The ratio between the lengths $Stub$ and W_p systematically affects the impedance of the radiator at the input of the feeding line, where W_p is the width of the patch.

The design procedure was to determine a set of initial values for the antenna parameters. The initial values of the radiator are W_p and L_p.

The design procedure consists of determining a set of initials values of the radiator W_p and L_p [24]. Initial values can be determined using the following formula (2-4):

$$W_p = \frac{c}{2f_r}\sqrt{\frac{2}{\epsilon_r + 1}} \tag{2}$$

$$\varepsilon_{eff} = \frac{\varepsilon_r + 1}{2} + \frac{\varepsilon_r - 1}{2}\left(\sqrt{1 + 12\frac{h}{W_p}}\right)^{\frac{-1}{2}} \tag{3}$$

$$L_p + \Delta L = \frac{c}{2f\sqrt{\epsilon_{ref}}} \tag{4}$$

Where,

$$\Delta L = 0.412h\frac{(\epsilon_{ref} + 0.3)}{(\epsilon_{ref} + 0.258)}\frac{(\frac{W_p}{h} + 0.264)}{(\frac{W_p}{h} + 0.8)} \tag{5}$$

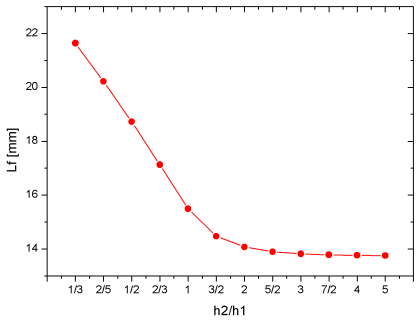

Fig. 3. Value of L_f by varying h_2/h_1.

Where, ϵ_{ref} is the effective dielectric constant value of the substrate, W_p is the width of the micro-strip line, h is the thickness value of the substrate and ΔL is the extension value of the effective length due to the peripheral electromagnetic fields. So, the fringing capacitance (C_f) can be computed using the formula.

$$C_f = \frac{\Delta L\sqrt{\epsilon_{ref}}}{cZ_0} \tag{6}$$

Where Z_0 the characteristic input impedance of the line and c is the speed of light value $c = 3.10^8 ms$. The starting value used for the length of the feed line under the radiator was $Stub = \frac{L}{2}$, a favorable condition for a maximum signal coupling [20].

For the purpose of impedance matching at 50Ω , the integrated line length L_f is designed to operate as a quarter-wavelength impedance transformer. The length L_f was computed using Eq. 7, where ϵ_{ref} is the effective dielectric constant value of the incorporated line [25].

$$L_f = \frac{c}{4f\sqrt{\epsilon_{ref}(1 - e^{\frac{-1.55h_2}{h_1}})}} \tag{7}$$

The value of L_f by varying h_2/h_1 is graphically shown in the following Figure (see Fig. 3). The choice of h_1 and h_2 was chosen to improve the mechanical and technical antenna performance. In this case, the dimensions $h_1 = 3.2\ mm$ and $h_2 = 1.6\ mm$ are taken.

III. Reconfigurable Antenna Design and Configuration

The proposed antenna is composed of three rotating narrow-band patches mounted next to each other in the form of three square patch using the no contacting proximity feeding technique. See Fig. 4 and Fig. 5. Top view and the bottom view of this new design of the given antenna are presented respectively by the. Fig. 6 and Fig. 7. The antenna is printed on a denim substrate of 68.8 mm x 98 mm x 4.8 mm with a dielectric constant of 1.77 and a height of 1.6 mm.

The work presented in [25], gives us the experimental electrical characteristics of the denim used in this design, resulting dielectric constant is $\epsilon_r = 1.77$ and loss tangent $tan\ \delta$

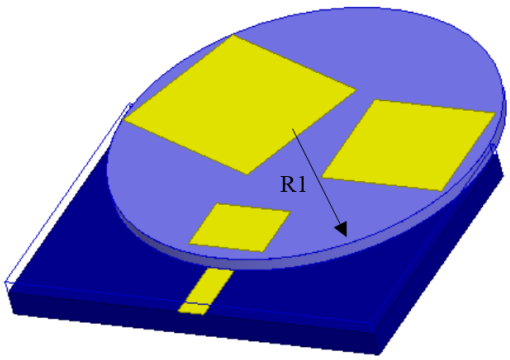

Fig. 4. The proposed antenna in 3D.

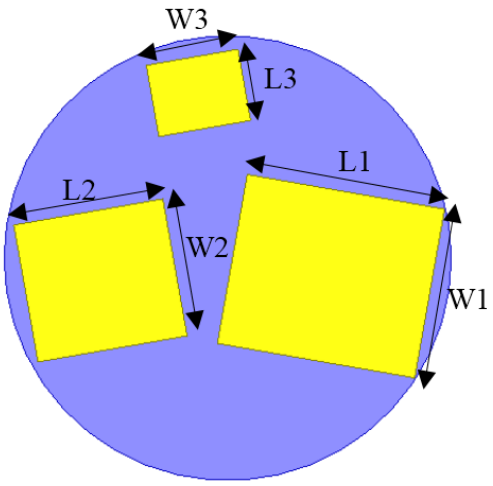

Fig. 5. Three shapes patch module.

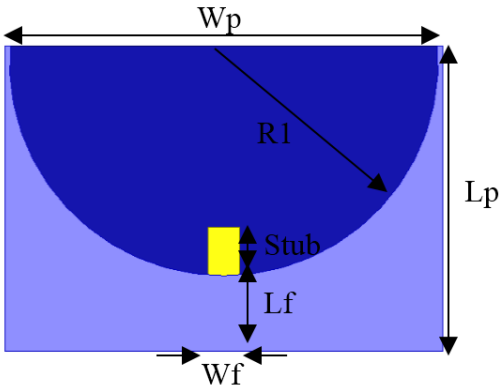

Fig. 6. Top view of the proposed antenna.

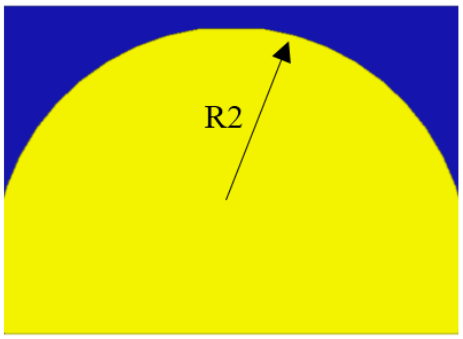

Fig. 7. Bottom view of the proposed antenna.

$= 0.05$ (intrinsic characteristic of the material). The thickness of the substrate was measured along a denim sample area of 10 mm x 10 mm using a caliper, resulting in an average value of 0.7 mm. The characteristics of PCPTF were given by the maker: electrical conductivity $\sigma = 2.5{\times}10^5\ s/m$ and thickness value $t = 0.08mm$.

The antenna is composed of patches with similar geometric shapes, in this work they are three square patches, printed on a 48 mm radius circular substrate. The patches are powered by a proximity feed of dimensions 7 mm x 19 mm. The dimensions of the patches are computed and optimized to work at the desired time in well-defined frequency bands. In our case, these are WLAN, WiMAX or Bluetooth bands.

The shape and position of the antenna patches are optimized using a parametric analysis using a numerical platform such as finite element method. The resonance frequency is obtained by a mechanically rotating the shape of the desired patch above the micro-strip line. At each rotation step (0 degree, 110 degree and 200 degree), a different patch is excited and a different resonant frequency is obtained (all possible configurations are detailed in the Fig. 8).

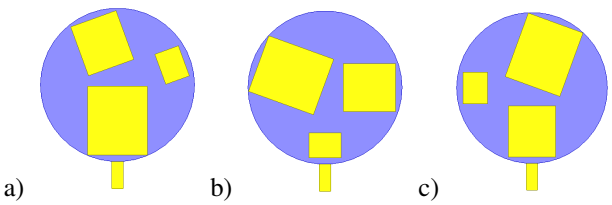

Fig. 8. Antenna configurations, a) at Position 1, b) at Position 1, c) at Position 3.

The circular substrate is rotated via a bipolar step-by-step engine attached below the antenna. The rotating part of the bipolar step-by-step engine is a cylinder of length 10 mm and diameter 10 mm. Table I illustrates the different dimensions of the proposed work after a series of numerical optimization.

A. Analysis of the Proposed Antenna

The Figures 12, 13 and 14 clearly show that when the length Stub is decreased, the resonance frequency shifts to the left

TABLE I
DIMENSIONS IN MM OF THE PROPOSED WORK.

Parameter	Symbol	Dimension (mm)
Micro-strip width	W_f	7
Micro-strip length	L_f	12
feed line inset width	$Stub$	7
Patch 1 width	W_1	37
Patch 1 length	L_1	43
Patch 2 width	W_2	30
Patch 2 length	L_2	27.5
Patch 3 width	W_3	20
Patch 3 length	L_3	15.6
Rotatable module radius	R_1	48
Ground radius	R_2	50
Substrate width	W_p	98
Substrate length	L_p	68.8
Substrate 1 height	h_1	3.2
Substrate 2 height	h_2	1.6

side and vice versa with a slight variation on the value of the return loss.

In another way, increasing the W_f width value for the Bluetooth band creates a radio interference band around 5 GHz (see Fig. 15). To eliminate this problem we took a value of $W_f = 7mm$.

For the WLAN band, it can be seen from Fig. 16 that the increase in the value of W_f clearly improves the value of the reflection coefficient. Inverted behavior is observed at the WiMAX band. See Fig. 17.

B. Proposed Antenna

The final configurability of the antenna, proposed in this work, can be seen from the return loss results presented in Fig. 9. The antenna has the ability to tune [2.2782 - 2.5233] GHz at the resonance frequency 2.4 GHz (The antenna is rotated by 0 to get the position 1), [5.4881-6.2095] GHz at the resonance frequency 5.83 GHz (The antenna is rotated by 110 to get the position 2), [3.3391-3.7423] GHz at the resonance frequency 3.55 GHz (The antenna is rotated by 200 to get the position 3).

The Figure 10 shows that VSWR<2 (Voltage Standing Wave Ratio) has been successfully achieved at required resonance three bands ($VSWR_1 = 1.21$ at 2.4 GHz (first band), $VSWR_2 = 1.08$ at 3.55 GHz (second band) and $VSWR_3 = 1.09$ at 5.83 GHz (third band)).

The calculated gain of the antenna proposed in different operating states is shown in Fig. 11. The gain is calculated on discrete frequencies belonging to the desired WLAN, WiMAX and Bluetooth bands. The computed values are very satisfying and concurrent compared to other published works.

The electromagnetic radiation pattern of the frequency reconfigurable antenna in the XZ plane ($\Phi = 0^o$) and the YZ plane ($\Phi = 90^o$) at the resonance frequencies 2.4 GHz, 5.83 GHz and 3.55 GHz are presented respectively in Fig. 18, 19 and 20. For all positions, it can be seen that the antenna shows a quasi-omnidirectional radiation pattern with

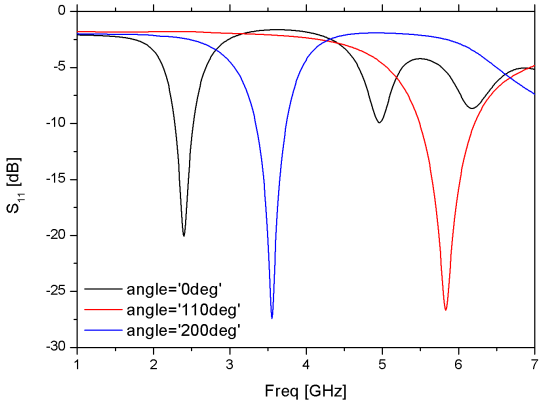

Fig. 9. Return loss by varying the frequency of the proposed antenna.

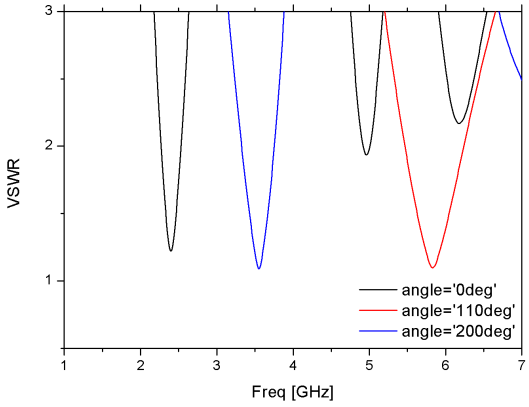

Fig. 10. VSWR by varying the frequency of the proposed antenna.

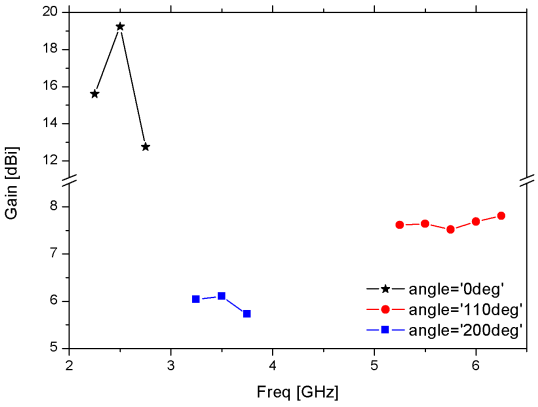

Fig. 11. Gain vs frequency at different states.

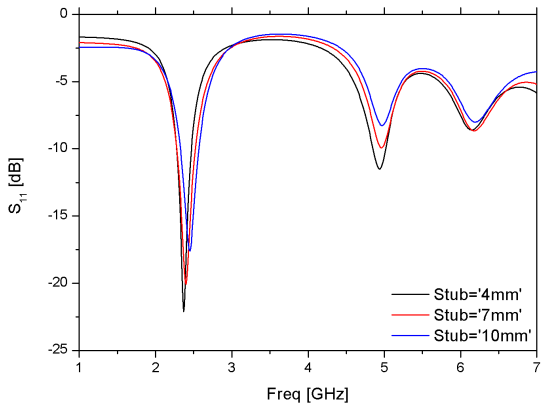

Fig. 12. Return loss values vs frequency by varying $Stub$ at position 1.

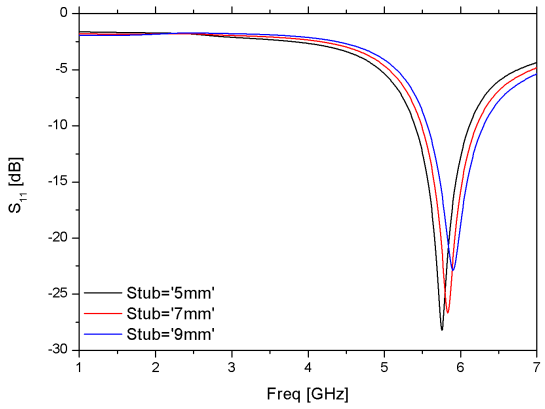

Fig. 13. Return loss values vs frequency by varying $Stub$ at position 2.

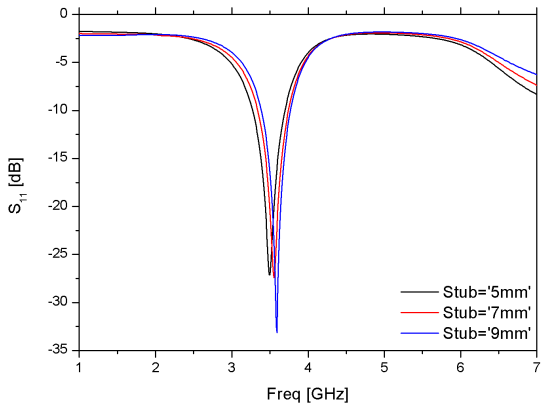

Fig. 14. Return loss values vs frequency by varying $Stub$ at position 3.

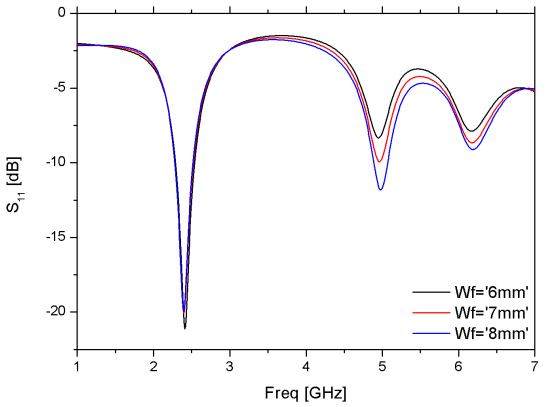

Fig. 15. Return loss values vs frequency by varying W_f at position 1.

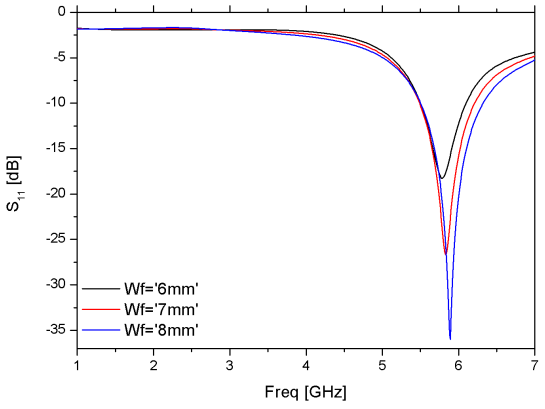

Fig. 16. Return loss values vs frequency by varying W_f at position 2.

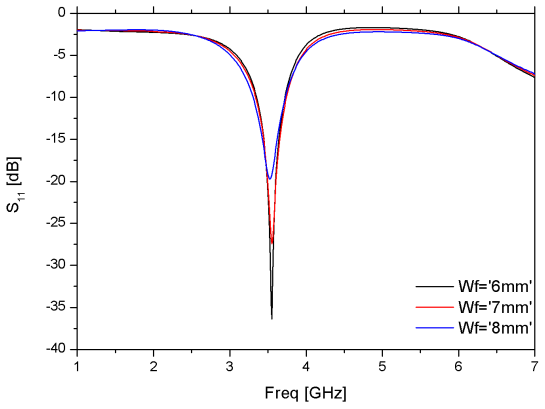

Fig. 17. Return loss values vs frequency by varying W_f at position 3.

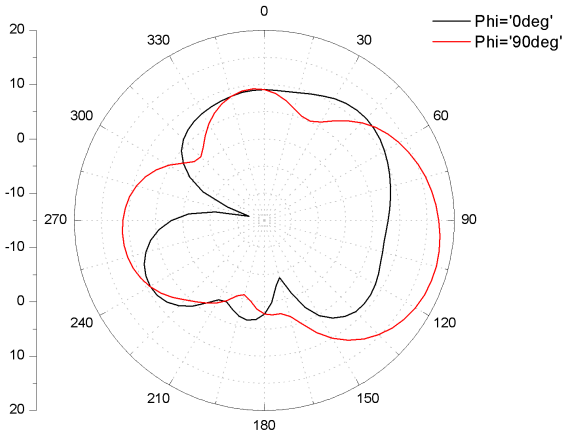

Fig. 18. Radiation pattern at 2.4 GHz (position 1).

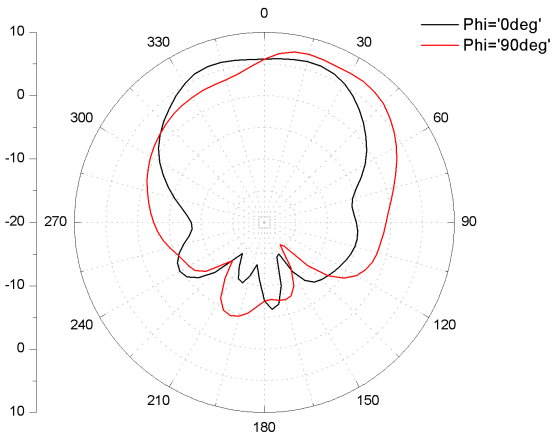

Fig. 19. Radiation pattern at 5.83 GHz (position 2).

a small distortion and therefore keeps the characteristics of the radiation of an ordinary patch antenna.

Table II summarizes the final results of the proposed antenna at different positions. We can deduce that the three frequency bands completely cover the commercialized bands intended for WLAN, WiMAX and Bluetooth.

TABLE II
PERFORMANCE OF THE PROPOSED ANTENNA.

Performance	Position 1	Position 2	Position 3
Application	Bluetooth	WLAN	WiMAX
Frequency [GHz]	2.4	5.83	3.55
Return Loss [dB]	-20.08	-26.67	-27.42
BW fr_1-fr_2 [GHz]	2.2782- 2.5233	5.4881-6.2095	3.3391-3.7423
BW [MHz]	245	721	403
BW [%]	10.2	12.37	11.35
Gain [dBi]	17.78	7.48	6.06

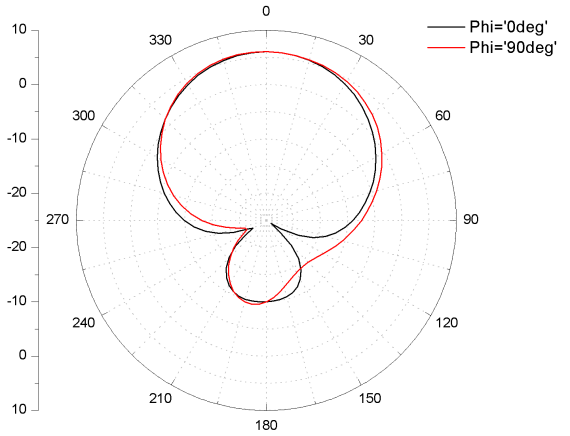

Fig. 20. Radiation pattern at 3.55 GHz (position 3).

C. Comparison Between the Proposed Antenna and Previous Work

The proposed antenna is compared with some recently published works in the same bands, a brief comparison is presented in Table III. Table III shows that [26] and [27] use FR4 epoxy as a substrate with a thinner thickness than our antenna which uses denim as a substrate with a very thick thickness. For the three bands, we can conclude that the proposed antenna shows better performance and achieves a much higher gain and offers bandwidth similar to the works cited above. Also, we see from [26] that large number of PIN diodes increases the insertion loss and then affects the performance of the antenna.

IV. CONCLUSION

In this paper a reconfigurable frequency antenna has been designed for commercial applications. The design was based on a non-contact feeding by rotating three square patches to avoid contact coupling problems. The servocontrol is achieved thanks to a bipolar step-by-step engine to obtain the required position. The value of the antenna parameters mentioned above was determined using a numerical platform with a discretization of 0.01 GHz for the calculation of the frequency at different states.

The results obtained proves that the proposed antenna operates efficiently in the desired bands and has a good quasi-omnidirectional radiation. It is characterized by great simplicity, compactness, reconfigurability and flexibility that makes it a promising candidate for WLAN, WiMAX and Bluetooth applications. In a very near future, we will try to validate experimentally the results obtained as well as the miniaturization of the proposed rotating antenna.

REFERENCES

[1] Y.-Y. Lin and T.-G. Ma, "Frequency-reconfigurable self-oscillating active antenna with gap-loaded ring radiator," *IEEE Antennas and Wireless Propagation Letters*, vol. 12, pp. 337–340, 2013.

TABLE III
COMPARISON WITH PREVIOUSLY SIMILAR PUBLISHED WORKS.

Characteristics	[26]	[27]	This work
Configurability type	PIN switches	Multiband	Rotatable antenna
No of PIN switches	3	0	0
Feeding technique	Micro-strip line	Proximity feeding	Proximity feeding
Substrate	FR4 Epoxy	FR4 Epoxy	Denim
Thickness $[mm]$	0.8	1.6	4.8
Bluetooth band $[GHz]$	2.3-2.51	2.4-2.485	2.28 - 2.523
Bluetooth WB $[MHz]$	210	85	245
Bluetooth Gain $[dBi]$	0.8	< 2	17.78
WiMAX band $[GHz]$	3.35-3.75	3.33.7	3.339-3.742
WiMAX WB $[MHz]$	400	400	403
WiMAX Gain $[dBi]$	1.5	< 3	7.48
WLAN band $[GHz]$	4.95-5.53	55.95	5.488-6.21
WLAN WB $[MHz]$	580	950	721
WLAN Gain $[dBi]$	1.8	< 4	6.06

[2] H. Boudaghi, M. Azarmanesh, and M. Mehranpour, "A frequency-reconfigurable monopole antenna using switchable slotted ground structure," *IEEE Antennas and Wireless Propagation Letters*, vol. 11, pp. 655–658, 2012.

[3] A. Valizade, P. Rezaei, and A. A. Orouji, "Design of reconfigurable active integrated microstrip antenna with switchable low-noise amplifier/power amplifier performances for wireless local area network and wimax applications," *IET Microwaves, Antennas & Propagation*, vol. 9, no. 9, pp. 872–881, 2015.

[4] A. Valizade, M. Ojaroudi, and N. Ojaroudi, "Cpw-fed small slot antenna with reconfigurable circular polarizion and impdeance bandwidth characteristcis for dcs/wimax applications," *Progress In Electromagnetics Research*, vol. 56, pp. 65–72, 2015.

[5] M.-C. Tang and R. W. Ziolkowski, "Compact hyper-band printed slot antenna: Design and experiments," in *Antennas and Propagation (EuCAP), 2014 8th European Conference on*. IEEE, 2014, pp. 594–596.

[6] B. Badamchi, A. Valizade, P. Rezaei, and Z. Badamchi, "A reconfigurable square slot antenna with switchable single band, uwb, and uwb with band notch function performances," *Appl. Comput. Electromagn. Soc.(ACES) J*, vol. 29, no. 5, 2014.

[7] B. Badamchi, J. Nourinia, C. Ghobadi, and A. V. Shahmirzadi, "Design of compact reconfigurable ultra-wideband slot antenna with switchable single/dual band notch functions," *IET Microwaves, Antennas & Propagation*, vol. 8, no. 8, pp. 541–548, 2014.

[8] M. N. M. Kehn, Ó. Quevedo-Teruel, and E. Rajo-Iglesias, "Reconfigurable loaded planar inverted-f antenna using varactor diodes," *IEEE Antennas and Wireless Propagation Letters*, vol. 10, pp. 466–468, 2011.

[9] X. Yang, J. Lin, G. Chen, and F. Kong, "Frequency reconfigurable antenna for wireless communications using gaas fet switch," *IEEE Antennas and Wireless Propagation Letters*, vol. 14, pp. 807–810, Dec 2015.

[10] E. R. Brown, "Rf-mems switches for reconfigurable integrated circuits," *IEEE Transactions on Microwave Theory and Techniques*, vol. 46, no. 11, pp. 1868–1880, Nov 1998.

[11] Y. Xu, Y. Tian, B. Zhang, J. Duan, and L. Yan, "A novel rf mems switch on frequency reconfigurable antenna application," *Microsystem Technologies*, pp. 1–9, 2018.

[12] G. Chen, X. Yang, and Y. Wang, "Dual-band frequency-reconfigurable folded slot antenna for wireless communications," *IEEE Antennas and Wireless Propagation Letters*, vol. 11, pp. 1386–1389, 2012.

[13] I. Bahl, P. Bhartia, and S. Stuchly, "Design of microstrip antennas covered with a dielectric layer," *IEEE Transactions on Antennas and Propagation*, vol. 30, no. 2, pp. 314–318, 1982.

[14] K. Carver and J. Mink, "Microstrip antenna technology," *IEEE transactions on antennas and propagation*, vol. 29, no. 1, pp. 2–24, 1981.

[15] G. Gronau and I. Wolff, "Aperture-coupling of a rectangular microstrip resonator," *Electronics Letters*, vol. 22, no. 10, pp. 554–556, 1986.

[16] J. R. James and P. S. Hall, "Handbook of microstrip antennas. volumes 1 & 2," *NASA STI/Recon Technical Report A*, vol. 90, 1989.

[17] P. Katehi and N. Alexopoulos, "On the modeling of electromagnetically coupled microstrip antennas–the printed strip dipole," *IEEE transactions on antennas and propagation*, vol. 32, no. 11, pp. 1179–1186, 1984.

[18] D. M. Pozar, "Microstrip antenna aperture-coupled to a microstripline," *Electronics letters*, vol. 21, no. 2, pp. 49–50, 1985.

[19] ——, "Microstrip antennas," *Proceedings of the IEEE*, vol. 80, no. 1, pp. 79–91, 1992.

[20] D. M. Pozar and B. Kaufman, "Increasing the bandwidth of a microstrip antenna by proximity coupling," *Electronics letters*, vol. 23, no. 8, pp. 368–369, 1987.

[21] A. Elfatimi, S. Bri, and A. Saadi, "Comparison between techniques feeding for simple rectangular, circular and triangular patch antenna at 2.45 ghz," in *2018 4th International Conference on Optimization and Applications (ICOA)*, April 2018, pp. 1–5.

[22] R. Garg, P. Bhartia, I. J. Bahl, and A. Ittipiboon, *Microstrip antenna design handbook*. Artech house, 2001.

[23] D. M. Pozar and D. H. Schaubert, *Microstrip antennas: the analysis and design of microstrip antennas and arrays*. John Wiley & Sons, 1995.

[24] C. a Balanis, "Antenna theory-analysis and design," 2005.

[25] M. Grilo and F. S. Correra, "Rectangular patch antenna on textile substrate fed by proximity coupling," *Journal of Microwaves, Optoelectronics and Electromagnetic Applications (JMOe)*, vol. 14, pp. 103–112, 2015.

[26] M. Borhani, P. Rezaei, and A. Valizade, "Design of a reconfigurable miniaturized microstrip antenna for switchable multiband systems," *IEEE Antennas and Wireless Propagation Letters*, vol. 15, pp. 822–825, 2016.

[27] P. S. Bakariya, S. Dwari, M. Sarkar, and M. K. Mandal, "Proximity-coupled microstrip antenna for bluetooth, wimax, and wlan applications," *IEEE Antennas and Wireless Propagation Letters*, vol. 14, pp. 755–758, 2015.